Note on chaos and diffusion

C. P. Dettmann
University of Bristol, Department of Mathematics, Bristol BS8 1TW, UK

E. G. D. Cohen
The Rockefeller University, 1230 York Ave, New York NY 10021, USA
(November 14, 2000)

Using standard definitions of chaos (as positive Kolmogorov-Sinai entropy) and diffusion (that multiple time distribution functions are Gaussian), we show numerically that both chaotic and nonchaotic systems exhibit diffusion, and hence that there is no direct logical connection between the two properties. This extends a previous result for two time distribution functions.

I. INTRODUCTION

It is generally surmised that microscopic chaos is a necessary condition for diffusive behavior of a system. Microscopic chaos here means a positive Kolmogorov-Sinai (KS) entropy, or equivalently, at least one positive Lyapunov exponent. While this seemed to be confirmed by an ingenious experiment with a Brownian particle [1], we showed that the same behavior on which the microscopic chaoticity of the Brownian system was established also held for a manifestly nonchaotic system with zero KS entropy [2,3], so that both systems exhibited diffusion.[1] In these works we used the mean square displacement (Eq. 3 below), a two time distribution function, as our definition of diffusion.

An anonymous referee of a Ref. [3], alerted us to a definition of diffusion (Eq. 1) which involved multitime distribution functions and the question arose whether those could distinguish between chaotic and nonchaotic models, in that all our chaotic models and none of our nonchaotic models would satisfy this definition. In this note we show that this behavior does not occur: no difference has been found between the diffusive behavior of microscopically chaotic and nonchaotic models even in the multitime distribution functions we studied.

Our models, a subset of those of Ref. [3], consist of a point particle moving with unit speed in two dimensions, undergoing specular reflections (collisions) with fixed non-overlapping scatterers. The shapes, positions, and orientations of the scatterers in the various models are defined in the next section, and can be classified as Lorentz or (modified) Ehrenfest models. For each fixed configuration of scatterers, the particle's position $\mathbf{x}$ is determined numerically as a function of the time t for random initial positions $\mathbf{x}(0)$ (which are uniformly distributed over the plane, except that they cannot lie inside a scatterer) and random initial velocity directions (also uniformly distributed) of the particle. The probabilities below are defined with respect to this distribution of initial conditions.

The definition of diffusion proposed by the referee and used in this paper is stated in terms of the probability of the particle initially at the origin visiting n regions at n different specified times. Explicitly, a system is said to be diffusive, if, for all $n = 1, 2\ldots$, the $n+1$ time (including $t = 0$) probability distributions $\mathcal{P}$ satisfy the relation [7]:

$$\begin{aligned}\lim_{\lambda\to\infty} &\mathcal{P}(\mathbf{x}(\lambda^2 t_1)\in\lambda\mathcal{D}_1, \mathbf{x}(\lambda^2 t_2)\in\lambda\mathcal{D}_2,\ldots,\mathbf{x}(\lambda^2 t_n)\in\lambda\mathcal{D}_n|\mathbf{x}(0)=0)\\ &=\int_{\mathcal{D}_1}d\mathbf{x}_1\int_{\mathcal{D}_2}d\mathbf{x}_2\ldots\int_{\mathcal{D}_n}d\mathbf{x}_n p(\mathbf{x}_1,t_1)p(\mathbf{x}_2-\mathbf{x}_1,t_2-t_1)\ldots p(\mathbf{x}_n-\mathbf{x}_{n-1},t_n-t_{n-1}) \end{aligned}\tag{1}$$

where $0 < t_1 < t_2 < \ldots < t_n$ are arbitrary times and the $\mathcal{D}_k$ $(k = 1, 2\ldots n)$ are arbitrary subsets of the plane. $p(\mathbf{x}, t)$ is the Gaussian Green's function of the (generally anisotropic) diffusion equation in two dimensions,

$$p(\mathbf{x},t)=\frac{e^{-u^2/4D_{uu}t-v^2/4D_{vv}t}}{4\pi\sqrt{D_{uu}D_{vv}}t}\tag{2}$$

and determines the probability density of a displacement $(\lambda u, \lambda v)$ in time $\lambda^2 t$ in the limit $\lambda\to\infty$. The scaling of the position and time by λ is based on the fact that for Gaussian diffusion the mean square displacement of the particle

[1]There are at least two integrable models (hence, with zero Lyapunov exponents) that have been shown to exhibit diffusion as defined by Eq. 1, a one dimensional hard rod model [4] and a heavy particle in a lattice of light particles [5]. In both cases there are an infinite number of moving particles, so we expect that the KS entropy is infinite, as in the infinite ideal gas [6]. Here we have only one moving particle, and we argued in Ref. [3] that the KS entropy of our nonchaotic models is zero.

is proportional to the time, and is a macroscopic limit. Here, u and v are distances measured in the eigendirections of the diffusion tensor, while D_{uu} and D_{vv} are the corresponding eigenvalues. In the isotropic case $D_{uu} = D_{vv} = D$ and the choice of orthogonal directions (u, v) is arbitrary.

The components of the diffusion tensor in an arbitrary orthonormal basis $\{\mathbf{e}_j\}$ (so that $\mathbf{x} = \sum_j x_j \mathbf{e}_j$) can be related to the mean square displacement $(i, j = 1, 2)$:

$$D_{ij} = \lim_{t\to\infty} \frac{\langle \Delta x_i \Delta x_j \rangle}{2t} \tag{3}$$

where $\Delta\mathbf{x} = \mathbf{x}(t) - \mathbf{x}(0)$. This expression involves the usual 2-time distribution function, that is, $n = 1$ in Eq. (1). The mean square displacement is discussed in Ref. [3], where we found numerically that both chaotic and nonchaotic models exhibited Gaussian diffusion. It is conceivable that a system may have Gaussian 2-time distribution functions but non-Gaussian multi-time distribution functions, i.e., for larger values of n. The results of this note show that also for larger n, both chaotic and nonchaotic models appear diffusive within the accuracy of the numerical methods.

II. MODELS

The models we consider are the same as some of those discussed in detail in Ref. [3].[2] As mentioned above, they all contain a point particle colliding with fixed non-overlapping scatterers in two dimensions. The density is such that the scatterers cover exactly half of the available area.

The microscopically chaotic models are Lorentz models, consisting of circular scatterers distributed in position either periodically or randomly over the plane, such that they do not overlap. They are microscopically chaotic as they have a positive KS entropy. See Fig. 1

The microscopically nonchaotic models are Ehrenfest-like models, consisting of square scatterers distributed in position either periodically or randomly over the plane, such that they do not overlap. They are microscopically nonchaotic, with zero KS entropy. Unlike the original Ehrenfest model, the squares in this paper are always oriented at random. See Fig. 1.

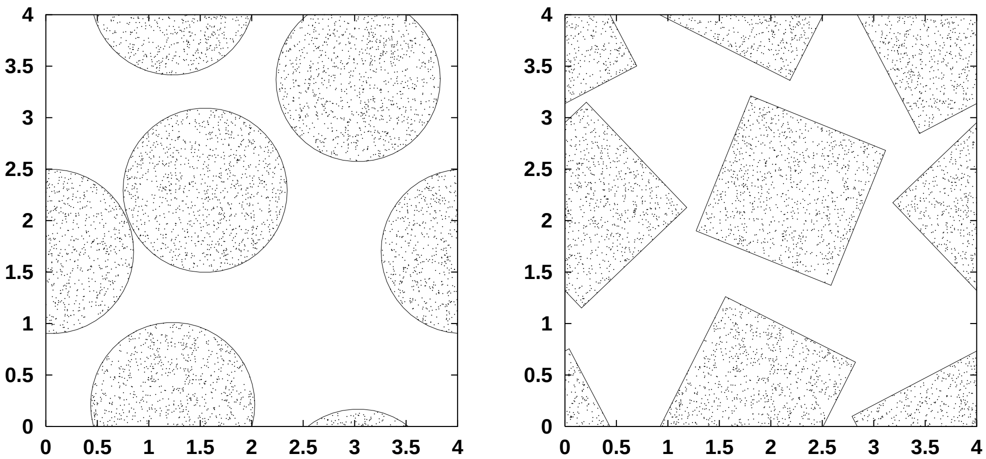

FIG. 1. The periodic Lorentz model (left) and periodic modified Ehrenfest model (right).

In both the Lorentz and Ehrenfest periodic models, the elementary cell is square and contains four scatterers. The random models have no preferred directions, so the diffusion is isotropic. In contrast, the periodic models have a directionality defined by the elementary cell, and the diffusion is anisotropic as in Eq. (2).

[2]Specifically: the periodic circles were denoted LP4 in [3], the randomly positioned circles L∞, the periodic squares RP4 and the randomly positioned squares R∞. Here, the L stands for the Lorentz gas, R for the random orientations of the squares, P for periodic, 4 for the linear dimension of the unit cell (there are also 4 scatterers per unit cell), and ∞ for the infinite "unit cell".

We investigated Eq. (1) for equally spaced times and two choices of the subsets $\mathcal{D}_k$ of the plane:

A The $\mathcal{D}_k$ ($k \le n$) are all balls of radius $\epsilon = 1/\sqrt{10}$ centered on the origin for $n = 1\ldots 7$.

B $n = 2$, where $\mathcal{D}_1^{(i)}$ and $\mathcal{D}_2^{(i)}$ are two balls of radius $\epsilon = 1/\sqrt{10}$ centered on randomly chosen points $\mathbf{x}_k^{(i)}$; $i = 1\ldots 7$ identifies the different members of our sample of seven configurations of the $\mathcal{D}_k^{(i)}$, see Table I.

i	$x_1^{(i)}$	$y_1^{(i)}$	$x_2^{(i)}$	$y_2^{(i)}$	Fig. 4 symbol
1	0.41867	-1.48764	-0.02481	-1.57956	plus
2	1.59402	0.87882	1.60281	1.68137	cross
3	-1.08755	1.54166	-1.54202	0.53732	star
4	0.90683	-0.60837	1.05771	1.39554	open square
5	-0.13815	-0.56351	2.23801	-0.43826	filled square
6	2.19919	1.04709	1.55045	0.49136	open circle
7	-0.85062	-0.70816	-2.74100	-2.03641	filled circle

TABLE I. Positions defining the centers of the $\mathcal{D}_k^{(i)}$ for case **B**, and corresponding symbols in Fig. 4 below.

In both cases the scale factor varied as $\lambda = 1\ldots 100$, expanding the times by λ^2 and the subsets $\mathcal{D}_k$ by λ as required by Eq. (1). In case **A** this means that as λ increases the $\mathcal{D}_k$ become larger circles centered on the origin, while in case **B** the $\mathcal{D}_k$ become larger but also move off to infinity. The time steps were a single time unit, so that $t_k = k$ ($k = 1\ldots n$), and the maximum length of a trajectory was $\lambda^2 t_n = 70000$ for $\lambda = 100$ and $n = 7$. We took 1000 trajectories of length 10^6 with different initial conditions. In order to get reasonable statistics without excessive computer time we considered of order 10^6 segments of length 7×10^4 along each trajectory, shifting the initial state on the trajectory by one time unit. The sample size was thus of order 10^9. Because these trajectory segments overlap and hence are not independent, the statistical error is difficult to estimate a priori; we find below that it is greatest for the periodic square model, which is not surprising given that it is expected to have the largest amount of correlation.

In **A** we are testing for the probability for the particle to return n times at regular intervals to near its starting point. The motivation is that while in nonchaotic systems, a trajectory can follow an almost periodic trajectory for a long time, leading to a power law decay of recurrences, in chaotic systems the decay of recurrences is exponential. The power law for nonchaotic systems could lead to correlations over long times, inconsistent with the uncorrelated diffusion of Eq. (1). The integrand in Eq.(1) is a product, so the successive time steps are conditionally independent. [3]

In **B** we consider alternative choices for the $\mathcal{D}_k$ in the (we think) unlikely event that the rather special case **A** has different long time behavior than the general case. Case **B** does not extract almost periodic orbits but it may reveal other ways in which correlations might be manifest at long times. [4]

III. RESULTS

We measured the following quantities for the cases **A** and **B** discussed above:

1. The probability $\mathcal{P}(n;\lambda;\{\mathcal{D}_k\})$ for various λ, n and $\mathcal{D}_k$ as discussed above. We often omit some of the arguments for simplicity.

---

[3]Case **A** is similar to the "almost periodic recurrence" method of Ref. [3], which showed a difference between chaotic and nonchaotic models by looking at the probability for return to near the starting point many times at regular intervals. The difference is that in Ref. [3] the size of the regions remained fixed as the time of return increased, while in this paper the $\mathcal{D}_k$ and the times are scaled by factors λ and λ^2, respectively.

[4]It would be somewhat impractical to go beyond $n = 2$ in case **B**: (a) the integral on the RHS would be of increasingly high dimension and hence hard to evaluate, and (b) the probabilities would be much lower so that the statistics would be very poor, see Fig. 4 below.

2. For case **A**, the conditional probability $\mathcal{P}_c(n+1|n;\lambda;\{\mathcal{D}_k\}) = \mathcal{P}(n+1)/\mathcal{P}(n)$ for the particle being in $\lambda\mathcal{D}_{n+1}$ given that it was in all the previous $\lambda\mathcal{D}_k$ for $k = 1\dots n$. Again, we often omit arguments for simplicity.

Eq. (1) actually makes two testable assertions: Does the limit on the left hand side (LHS) exist, and if so, is it equal to the right hand side (RHS)? The above measured quantities give information about the LHS and we are first interested in the large λ limit of these quantities; for the RHS we obtain the diffusion tensor from Eq. (3) (see Table II) and perform the integration numerically. This has only been carried out up to $n = 2$ (which is a four-fold integration). However, for larger n and case **A**, the right hand side is (to a very good approximation) multiplied by a constant factor for each additional repetition, [5] so the prediction is that the conditional probabilities become independent of n for large λ and n. In fact our result show this behavior already at the smallest values of n.

Model	D_{xx}	$D_{xy} = D_{yx}$	D_{yy}	D_{uu}	D_{vv}
Random squares	0.1480	-0.0009	0.1480	0.1489	0.1471
Periodic squares	0.2265	0.0383	0.1304	0.2400	0.1170
Random circles	0.2777	0.0005	0.2763	0.2779	0.2761
Periodic circles	0.3087	0.0434	0.2878	0.3429	0.2536

TABLE II. Components of the diffusion tensor computed in original coordinates (x, y) from Eq. (3), and then diagonalized to give the (u, v) values. Note that the randomly placed and oriented squares as well as the randomly placed circles are isotropic, with $D_{xy} = 0$ and $D_{xx} = D_{yy}$ within errors of about 0.001, while the periodic models are anisotropic and satisfy neither of these conditions.

The results are shown in Figs. 2-4 and Table III. For all n and $\{\mathcal{D}_k\}$ the $\mathcal{P}(\lambda)$ approach a constant (apart from statistical error) at large λ, indicating convergence of the limit in Eq. (1), see Fig. 2 for case **A** and Fig. 4 for case **B**. For case **A**, all the conditional probabilities approach the same constant indicating conditional independence of the multi-time probabilities as predicted by diffusion, see Fig. 3; an equivalent statement is that on a logarithmic scale, all the curves in Fig. 2 become equidistant at large λ. We have verified numerically that in both cases **A** and **B** the values of the constants as $\lambda \to \infty$ are consistent with their values as given on the RHS of Eq. (1), thus confirming the diffusive nature of all these models.

Model	$\mathcal{P}_c(2\|1)_{th}$	$\mathcal{P}_c(2\|1)$	$\mathcal{P}_c(3\|2)$	$\mathcal{P}_c(4\|3)$	$\mathcal{P}_c(5\|4)$
Random squares	0.1443	0.1457	0.1448	0.1437	0.1426
Periodic squares	0.1288	0.1392	0.1295	0.1113	0.1147
Random circles	0.0827	0.0831	0.0835	0.0810	0.0825
Periodic circles	0.0781	0.0785	0.0788	0.0780	0.0776

TABLE III. Conditional probabilities $\mathcal{P}_c(n+1|n)$. The second, "theoretical" column gives the values calculated from numerical integration of the RHS of Eq. (1). The other columns, derived from Fig. 3 by averaging over λ from 50 to 100, agree with the values from column 2, and do not depend on n, consistent with conditional independence in the underlying probability distribution. The differences in the periodic square model are almost certainly due to statistical errors, as in Figs. 2, 3.

[5] The approximation can perhaps be understood as follows. If we perform all but the last $\mathbf{x}_n$ integration, we are left with an integral over a function, say $f_n(\mathbf{x}_n)$. At the $n+1$ stage, we have f_{n+1} as a linear operator $\mathcal{L}$ (integral over a Gaussian kernel) acting on f_n. Assuming $\mathcal{L}$ is well behaved, the f_n approach a limiting form $\bar{f}\lambda_0^n$ as $n \to \infty$ where $0 < \lambda_0 < 1$ is the leading eigenvalue of $\mathcal{L}$ and $\bar{f}$ is the leading eigenfunction. Performing the last integration, we find that successive integrals differ by a factor of λ_0, leading to a vanishing probability for $n \to \infty$.

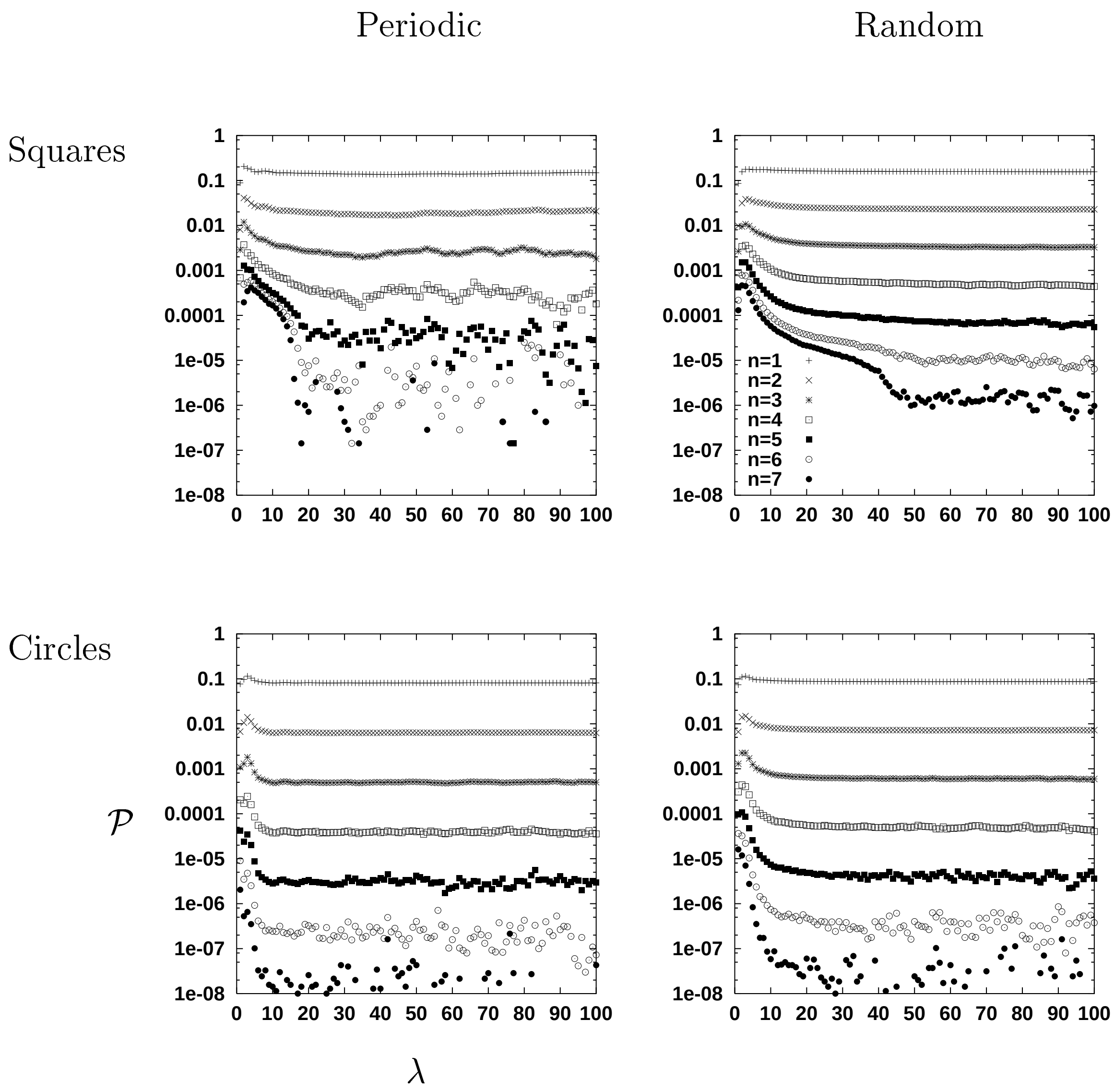

FIG. 2. Probabilities $\mathcal{P}(\lambda)$ as a function of λ for case **A**, with different curves giving $n = 1 \ldots 7$. Note that the probability becomes independent of λ indicating the existence of the limit on the LHS of Eq. (1). The equal spacing between subsequent values of n indicates a fixed ratio of successive recurrences since the scale is logarithmic. This is consistent with the uncorrelated diffusion as given by the RHS of Eq. (1). The statistical error is greatest when the probability is low, and when the correlations in the data are greatest, that is, for the periodic square model.

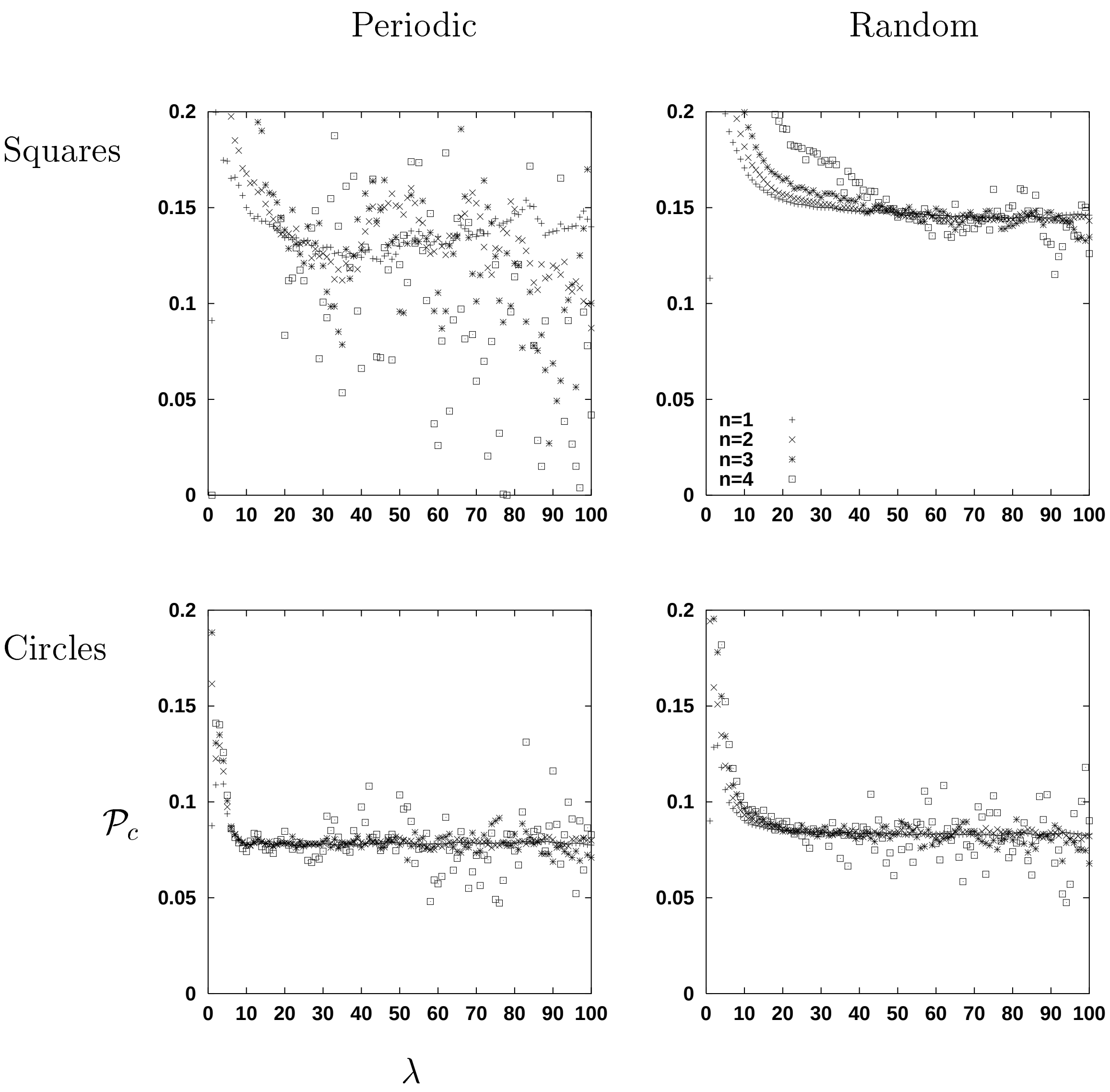

FIG. 3. Conditional probabilities $\mathcal{P}_c(n+1|n;\lambda)$ as a function of λ for case **A**, and $n = 1\dots4$, derived from Fig. 2. The equal spacing in Fig. 2 now causes the graphs corresponding to different values of n to coincide. Again, statistical error is greatest with low probability (larger n) and with greater correlations in the data (the periodic square model).

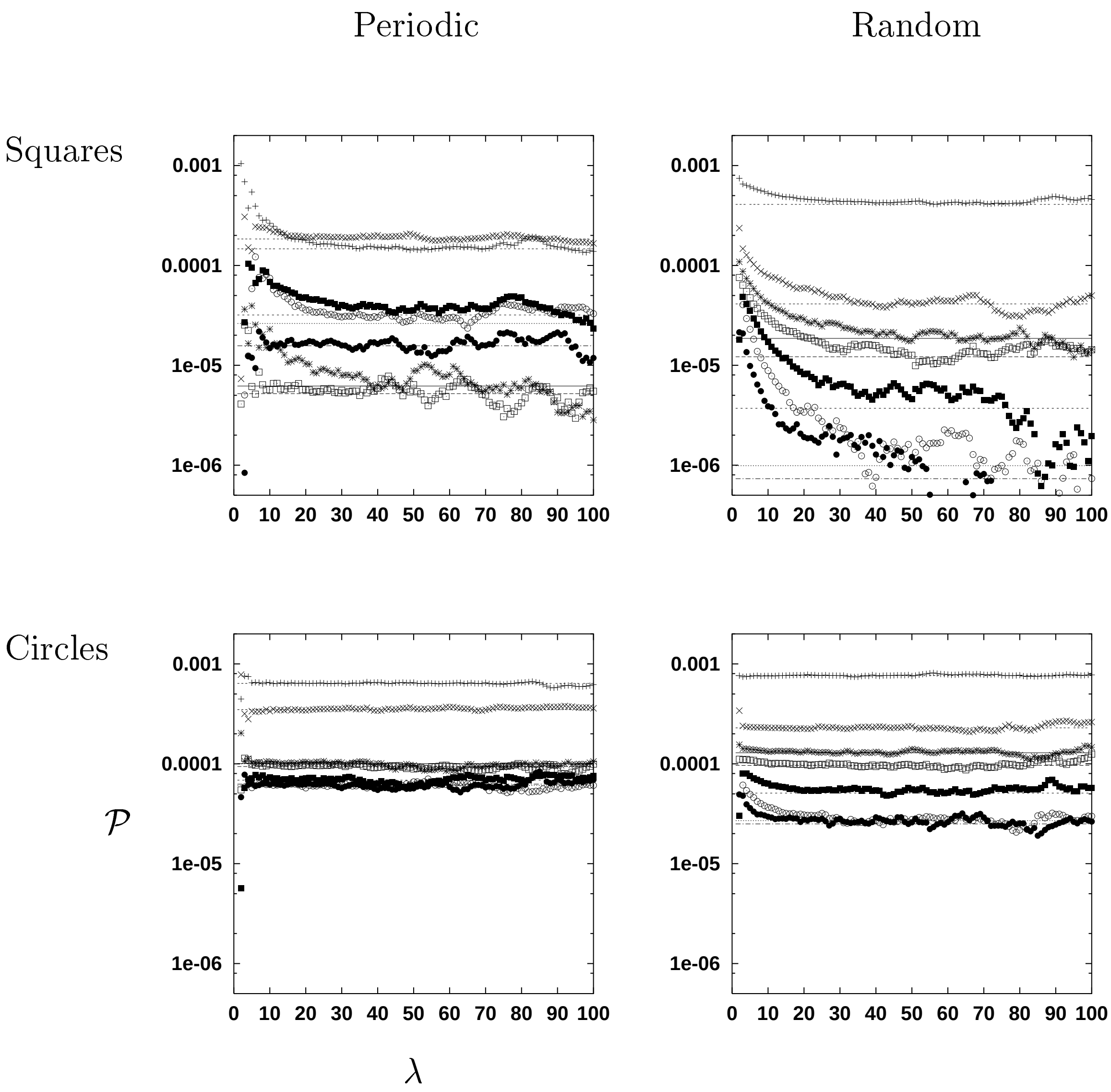

FIG. 4. Probabilities $\mathcal{P}(\lambda)$ as a function of λ for case **B**. The different symbols correspond to different $\mathcal{D}_k^{(i)}$ $(i = 1 \ldots 7)$ as given in Table I. The dashed or dotted horizontal lines give the predicted values from the RHS of Eq. (1), and are not visible when they run through the data. The order of the curves differ due to the anisotropy of the diffusion in the periodic models.

IV. DISCUSSION

1. The above mentioned results suggest that there is no difference in the diffusive behavior of chaotic (Lorentz) and non-chaotic (Ehrenfest) models. Both exhibit Gaussian diffusion and their only difference is the value of the diffusion coefficients.

2. The case **A**, in particular the larger probabilities for recurrence at small λ as seen in Fig. 2, especially suggests the presence of "small" periodic orbits, which favor return to previously visited regions for the nonchaotic wind-

tree models since they exhibit only algebraic $1/t$ decay (see Ref. [3]). For the chaotic Lorentz models, periodic orbits disappear exponentially fast in t and therefore more returns are less likely. Nevertheless this difference in periodic orbit stability, which indicates a more subtle chaotic difference than the corresponding KS entropies in these models, do not appear to lead to a qualitatively different, non-Gaussian, diffusion process.

3. The influence of small almost periodic orbits is clearly local and incoherent from region to region. It is therefore constantly wiped out and does not influence the global diffusion process at all, except for example in the values of the D_{ij}, which should decrease by a strong influence of almost periodic orbits.

4. Our results here appear to differ from the behavior observed in open (that is, finite with absorbing boundaries) Lorentz and Ehrenfest models in Ref. [3]. There, we studied the number of particles with different initial conditions remaining in the system as a function of time. Only the Lorentz model exhibited the exponential decay of particles characteristic of the diffusion equation; the Ehrenfest model corresponding to our squares exhibited $1/t$ decay due to trapping of particles around periodic orbits. This is not in contradiction to our results here (for which the nonchaotic model also exhibits diffusion) since the limits are different: With absorbing boundaries, the limit $t \to \infty$ occurs with the linear dimension of the observed region (the whole system) L fixed; in this note the linear dimension of the observed regions $\lambda\mathcal{D}$ is scaled as $t^{1/2}$, which is more natural for diffusion. Thus, the identification of a model with diffusion depends not only on the microscopic dynamics, but also on the manner in which the limit is taken. It would be interesting to investigate these relationships further.

5. To conclude, our results indicate that at least for the models we consider, subtle correlations, whether associated with almost periodic orbits in small clusters of scatterers or otherwise, are insufficient to modify the long time Gaussian form of the diffusion process when the natural macroscopic limit is taken (such that lengths are scaled with the squareroot of times). In so far as these correlations are determined by the microscopic chaotic nature of the system, the chaoticity does not seem to show up in the macroscopic diffusive behavior. This behavior is consistent with the results of the Brownian motion experiment discussed in Ref. [1], and the argument [2] that the long measuring times of 1/60s means that the results could come equally from chaotic or nonchaotic microscopic dynamics, and that any experimental determination of microscopic chaoticity would necessarily involve measurements at microscopic time scales.

ACKNOWLEDGMENTS

The authors are grateful to a referee of a previous paper [3] for making the important suggestion discussed in this paper. They also acknowledge the support of the Engineering Research Program of the Office of Basic Energy Sciences of the US Department of Energy under contract number DE-FG02-88-ER13847.

[1] P. Gaspard, M. E. Briggs, M. K. Francis, J. V. Sengers, R. W. Gammon, J. R. Dorfman, and R. V. Calabrese, Nature **394**, 865 (1998).

[2] C. P. Dettmann, E. G. D. Cohen and H. van Beijeren, Nature **401**, 875 (1999).

[3] C. P. Dettmann and E. G. D. Cohen, J. Stat. Phys. (in press); nlin.CD/0001062

[4] J. L. Lebowitz and J. K. Percus, Phys. Rev. **155**, 122 (1967); J. L. Lebowitz, J. K. Percus and J. Sykes, Phys. Rev. **171**, 224 (1968).

[5] R. J. Rubin, J. Math. Phys. **1**, 309 (1960); ibid **2**, 373 (1961).

[6] S. Goldstein, J. L. Lebowitz, and M. Aizenman, Lecture Notes in Phys. **38**, 112 (Springer, Berlin, 1975).

[7] J. R. Norris, "Markov chains" (Cambridge University Press, 1997).